Journal of the Persian Gulf
(Marine Science)/Vol. 3/No. 10/December 2012/6/1-6

Numerical Study on Resistance of a Bulk Carrier Vessel Using CFD Method

Ebrahimi, Aboozar

1- Faculty of Marine Engineering, Chabahar Maritime University, Chabahar, IR Iran

Received: July 2012 *Accepted: November 2012*

Abstract

Bulk carriers have an important role in international maritime transport. In this paper, we carried out a numerical study on a model of bulk carrier vessel and calculated total resistance of the model. A model of a bulk carrier vessel with length of 2.76 m, breadth of 0.403 m and draught of 0.173 m was selected for numerical modeling. Numerical work was done by commercial CFD software ANSYS FLUENT 13 based on finite volume method (FVM). Applying VOF model, FLUENT solved RANS equations and accordingly, free surface waves around vessel and total resistance were calculated. A fully structured mesh was used which generated in GAMBIT pre-processing software. Numerical solution was done for 5 different speeds from 0.2 to 0.95 m/s. Also, mesh dependency was studied by using four mesh sizes and finally, a mesh with 755,000 hexahedral cells was selected for all speeds. For verification of numerical results, experimental data from test of bulk carrier model were used. Model tests were carried out in towing tank of Galati University in Romania. Moreover, free surface waves from numerical study were compared with waves captured from model tests. The results showed that CFD results had an error up to 12 % relative to model test results and wave patterns around vessel were very similar to that of model test.

Keywords: *Bulk Carrier Vessel, Resistance, CFD, FLUENT, Model Test*

1. Introduction

Bulk carriers contribute to a substantial portion of world maritime transport. The world's bulk transport reached immense proportions in 2005 in which, 1.7 billion metric tons of coal, iron ore, grain, bauxite, and phosphate were transported by bulk carrier ships (UNCTAD, 2006). Today, the world's bulker fleet includes 6,225 ships of over 10,000 tons deadweight and represents 40% of all ships in terms of tonnage and 39.4% in terms of vessels.

* *E-mail: ab_ebrahimi@cmu.ac.ir*

In recent years, the numerical solution method and specially Computational Fluid Dynamic method (CFD) have developed for studying hydrodynamics of ships. The CFD method in comparison with model test has great advantages, such as lower costs, accessibility and more visible details in results e.g., pressure and velocity contours, vectors and gradients. One of the important weaknesses of this method is that it is less accurate.

Therefore, experimental data should be used for verification of CFD results. In this study, we use CFD method for calculating resistance of a bulk carrier model and then, verify results by experimental data from model test.

Numerical study on resistance of a ship has been performed in several cases. Thornhill et al. (2003) used a finite volume code to simulate the flow around a planning vessel at steady speed through calm water, using 3D unstructured hybrid mesh. Force and moment data from the simulations were used in an iterative scheme to determine the dynamic equilibrium position of the model at selected speeds. Van et al. (1998) measured flow around a VLCC tanker model.

Ogiwara et al. (1994) carried out a study on series of 60 and calculated pressure distribution around its hull. Jones and Clarke (2010) used FLUENT code for numerical simulation of flow around a modern naval ship, DTMB 5415 and calculated waves and free surface around it.

Banks et al. (2010) calculated components of container ship resistance numerically. They used ANSYS CFX for numerical simulation and compared CFD results with experimental results. Hakan et al. (2007) modeled a ship hull by using FLUENT commercial code and calculated resistance of model. Finally, they compared numerical results with experimental data. Obreja et al. (2005) carried out a series of model tests in a bulk carrier vessel. In this study, we used results of these tests for verification of numerical results. Accordingly, we used the geometry of experimental model for numerical modeling.

2. Model Geometry

A model of a Panamax bulk carrier ship was used in this study, that was a 1:80 scale of full scale ship. The bulk carrier model is shown in Figure 1. The characteristics of the ship and of the model are presented in Table 1.

Fig. 1: Model of bulk carrier ship (Obreja et al., 2005)

Table 1: Full scale ship and model main characteristics (Obreja et al., 2005)

Main characteristics	Full scale ship	Model
Length of waterline (L_{WL})	220.915 [m]	2.761[m]
Length between perpendiculars (L_{BP})	217.30 [m]	2.716[m]
Breadth of waterline (B)	32.20 [m]	0.403[m]
Draught mean (D)	13.83 [m]	0.173[m]
Trim (t)	0 [m]	0 [m]
Volumetric displacement (∇)	82626 [m^3]	0.161 [m^3]
Block coefficient (CB)	0.837	0.837
Midship section coefficient (C_M)	0.995	0.995
Waterline coefficient (C_{WP})	0.923	0.923

3. Numerical Solution

In recent years, the CFD methods and application of these methods for hydrodynamic study of ships have developed. Although, this method in comparison with model test is less accurate, it can be used for studying details of flow characteristics, e.g. drag and lift forces, pressure and velocity contours and waves. In this study, free surface flow around a model was simulated using FLUENT CFD software. This commercial software solves Reynolds-Averaged Navier-Stokes (RANS) equations in computational domain and computes pressure and velocity in all nodes and accordingly calculates total resistance of model. For capturing surface waves around model, Volume of Fluid (VOF) method was used.

The VOF method simulates the motion of two fluids by solving a single set of momentum equations and tracking the volume fractions of each of the fluids throughout the domain. A volume fraction function was defined for each of the fluids in the simulation and was set to unity if the given fluid occupied a cell volume or was set to zero otherwise. When the interface between two fluids cut through a computational cell the value of the function for a particular fluid represented the fraction of the cell volume occupied by that fluid Jones and Clarke (2010).

Equations (1) and (2) were the incompressible RANS equations in tensor form and Equation (3) was the equation of volume fraction transport Peric and Ferziger (2002).

$$\frac{\partial(\rho U_i)}{\partial t}+\frac{\partial(\rho U_i U_j)}{\partial x_j}=-\frac{\partial P}{\partial x_i}+\frac{\partial}{\partial x_j}\left[\mu\left(\frac{\partial U_i}{\partial x_j}+\frac{\partial U_j}{\partial x_j}\right)\right]-\frac{\partial}{\partial x_j}\left(\rho\overline{u'_i u'_j}\right)+f_i \quad (1)$$

$$\frac{\partial U_i}{\partial x_i}=0 \quad (2)$$

$$\frac{\partial c}{\partial t}+\frac{\partial(cU_j)}{\partial x_j}=0 \quad (3)$$

The volume fraction c was defined as (V_{air}/V_{total}) and the fluid density, ρ, and viscosity, μ, were calculated as Hakan et al. (2007):

$$\rho=\rho_{air}c+\rho_{water}(1-c) \quad (4)$$

$$\mu=\mu_{air}c+\mu_{water}(1-c) \quad (5)$$

External forces applied to the fluid were represented as f_i, which include buoyancy forces due to differences in density and momentum sources. The effect of turbulence on the flow is represented in Equation (2) by the Reynolds stress tensor $\rho\overline{u'_i u'_j}$.

4. Computational Domain

The computational domain and its dimensions are displayed in (Figure 2). These dimensions were selected according to Van et al. (1998). The domain was defined by a cube volume which the model volume subtracted from it. According to VOF model, from the bottom of the domain to the initial water surface was occupied by the water and the rest by the air. The hull and flow field were symmetric about the center plane of model. Therefore, just half of computational domain was considered for numerical treatment and the symmetry boundary condition applied at center plane. This could increase rate of computations and reduce time of solution.

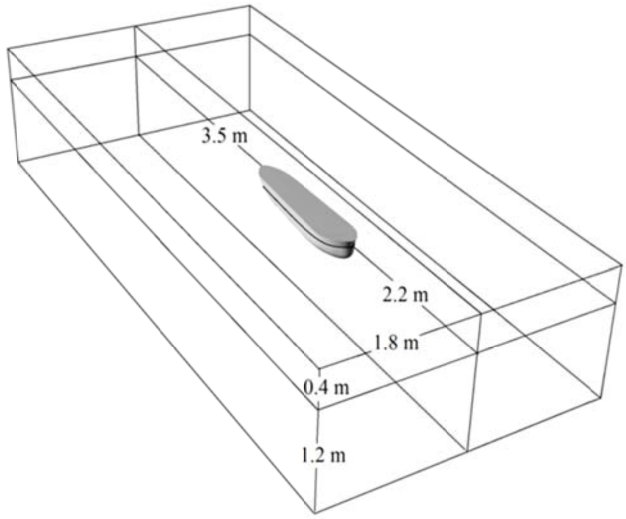

Fig. 2: Dimensions of computational domain

The GAMBIT Pre-processing software was used for mesh generation. A structured mesh was used in domain which all of the cells were hexahedral type. At stern and bow side of model and near free surface, meshes have refined in all states. For checking grid independency, we examined 4 grid sizes. By visual inspection of the wave pattern and detailed comparison of other results, such as pressure and velocity contours and resistance, we selected the optimum mesh. For example, total resistance of model due to different grid sizes is plotted in Figure 3 for V=0.9. It seemed by increasing grid size over 755000 cells, variation of resistance would be inconsiderable. Although, by using higher grid sizes, free surface waves could be captured more accurately. Finally, this size of mesh was selected for numerical modeling. Details of the grid are displayed in Figure 4.

A time-dependent solution with time step of 0.005 second was used for numerical solution. Monitoring of the resistance and free surface waves around model was used to know when the problem had reached a stationary solution. We observed that after 20 seconds, resistance of model and surface waves did not change considerablly. Therefore, this time was selected for modeling at all speeds. Numerical modeling was performed for 6 speeds between Fr = 0.09 (V=0.59 m/s) and Fr = 0.18 (V=0.95).

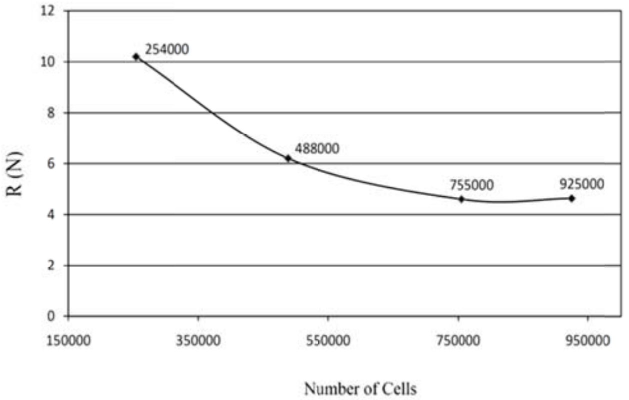

Fig. 3: Variation of resistance force due to mesh size

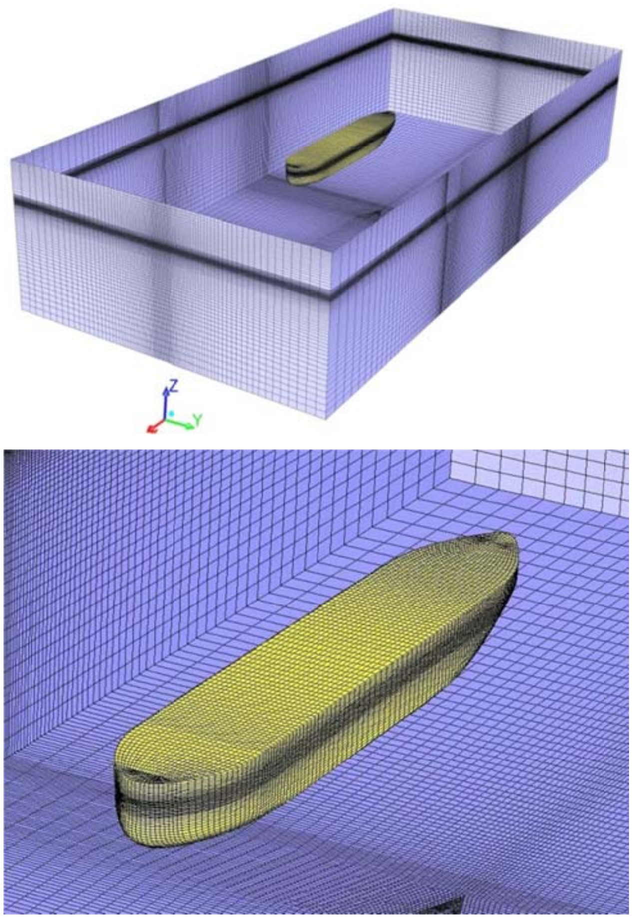

Fig. 4: Details of mesh

For turbulence modeling, standard, RNG and Realizable $k-\varepsilon$ models were used in numerical solution. Results showed that there was not much difference between results of these models, but the applied computing time for standard $k-\varepsilon$ model was shorter than that of others. Accordingly, standard $k-\varepsilon$ model was selected for numerical simulation. For near wall treatment, Standard Wall Functions were used. In numerical solution, trim and sinkage of model were kept fixed. Although, it could produce errors in results, but because of our limitations and complexity of 6-DOF modeling of hull, we applied this strategy. Also, because the vessel was displacement and Froude number was under 0.3, it seemed that this assumption was justifiable.

5. Boundary Conditions

The non-slip boundary condition was applied on the hull surface of the model, that is, the fluid particles on the body move with body velocity. Inlet and outlet of domain were divided into two boundaries by the initial location of free surface. At inlet, the upper part was entrance of air and the lower was for water. The velocity inlet condition was imposed to both parts. The static pressure at the outlet boundary was defined as a function of water volume fraction. The moving wall boundary condition was applied to side walls, top and bottom of domain and finally symmetry for center plane of domain. A variety of Pressure-Velocity Coupling schemes were available in FLUENT. The PISO scheme was selected at this study. For pressure and momentum spatial discretizations, body force weighted and second order upwind methods were selected, respectively.

The motion of the free surface flow was governed by gravitational force. Hence, the boundary conditions to be imposed must take into account the gravity effects. For this purpose, the computational domain was modeled as an open channel flow, which was also consistent with experimental setup.

6. Results and Discussion

6.1. Numerical Results

One way for verification of numerical results was comparing waves generated around model. The predicted waves around model of bulk carrier at speed of V=0.95 m/s and with available experimental data showed generally good agreement (Figures 5a and b). In these figures, wave systems of bow and stern were obvious.

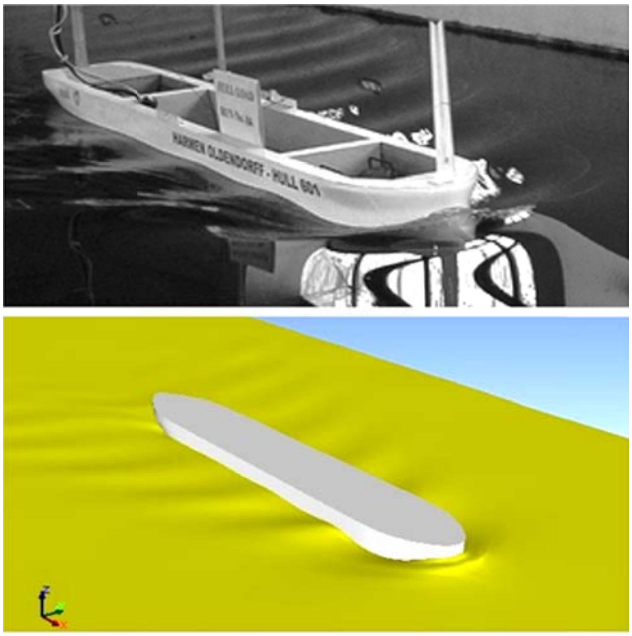

Figs. 5a (top) and b (bottom): Comparison of waves from CFD method and model test

The model test was an accurate and reliable method for measuring and investigating of the ship resistance. For verifying of numerical results in this study, we used results of model tests accomplished by (Obreja et al., 2005) in towing tank of Galati University.

The total resistance calculated by CFD method is shown in Figure 6 and compared with the experimental results.

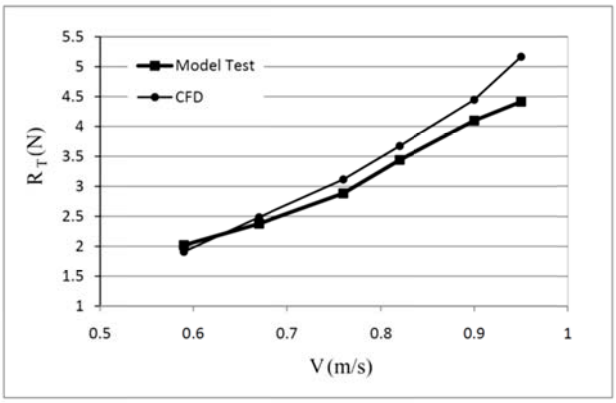

Fig. 6: Comparison of total resistance from CFD and model test

As shown in Figure 6, there was little difference between experimental and numerical findings. Total resistance of bulk carrier model from CFD method is up to 5 percent difference with experimental results in lower speeds, but after that, it reached to 13%. The reason of these errors may be weakness of this CFD code for calculating wave making resistance. However, in low speeds which wave making resistance had smaller magnitude; CFD results showed less difference with experimental results. We could seemingly reduce errors by using the modern computers for numerical modeling and using finer grids.

6.2. ITTC 57 Method

Another way for estimating resistance of a ship was applying common empirical formulas, such as ITTC 57 method. In this study, frictional resistance of model for comparison by CFD results were investigated. Frictional resistance of ship (RF) was calculated from Equation (6):

$$R_F = C_f(0.5\rho S V_m^{\ 2}) \tag{6}$$

Coefficient of frictional resistance (Cf) was computed by empirical formula presented by ITTC-57 as shown in Equation (7):

$$C_f = \frac{0.075}{(\log Rn - 2)^2} \tag{7}$$

In Figure 7, frictional resistance from ITTC 1957 method was compared with frictional resistance from CFD method and there was good correlation betwen them. In all speeds, there was about 8% difference between results.

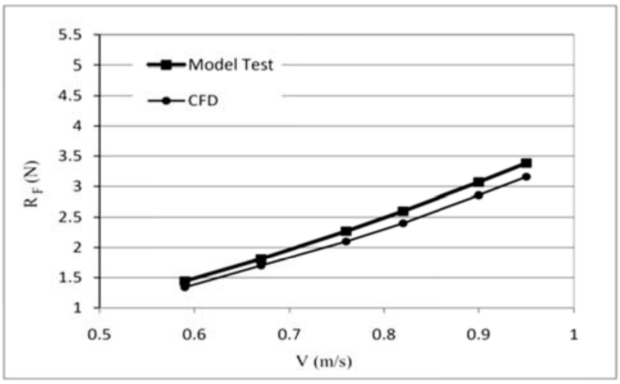

Fig. 7: Comparison of frictional resistance from CFD and ITTC 57 method

7. Conclusion

In this paper, an investigation was carried out on resistance of a bulk carrier vessel using CFD method by FLUENT software. Total resistance of model was calculated for different speeds and surface waves around model were obtained numerically. Finally, CFD results were compared with experimental data. Analysis showed that in low Froude numbers, CFD results had a difference up to 5% relative to the model test results. In higher Froude numbers, error increased up to 13%. The frictional resistance of model calculated by ITTC 57 method was compared with CFD results. There was good agreement between results of CFD and ITTC method.

References

Banks, J., Phillips, A. and Turnock, S., 2010. Free surface CFD prediction of components of ship resistance for KCS. 13th Numerical Towing Tank Symposium, Germany, pp.1-7.

Hakan, O., Bayraktar, S, and Yilmaz, T., 2007. Computational investigation of a hull, 2nd International Conference on Marine Research and Transportation, Italy, pp.145-150.

Jones, D.A., Clarke, D.B., 2010. Fluent code simulation of flow around a naval hull, the DTMB 5415. Technical report, Defense Science and Technology Organization. DSTO-TR-2465, 30P.

Obreja, D., Popescue, G, Ionas, O. and Pacuraru, F., 2005. Experimental techniques for vortices investigation around the ship model, Workshop on Vortex Dominated Flows, Romania.

Ogiwara, S. and Kajitani, H., 1994. Pressure distribution on the hull surface of series 60 model. Proceedings of CFD Workshop Tokyo, pp.350-358.

Peric, M., Ferziger, J.H., 2002. Computational Methods for Fluid Dynamics, Springer Pulication, 3rd edition, 426P.

Thornhill, E., Bose, N., Veitch, B. and Liu, P., 2003. Planing hull performance evaluation using a general purpose CFD code, 24th Symposium on Naval Hydrodynamics, the National Academy of Sciences, Japan.

United Nations Conference on Trade and Development (UNCTAD), 2006, 11 P.

Van, S.H., Kim W.J., Kim, D.H., Yim, G.T., Lee, C.J., and Eom, J.Y., 1998. Flow measurement around a 300K VLCC model. Proceedings of the annual spring meeting, Ulsan, pp.185-188.